

Molecular Dynamics Simulation of Polysulfone and Polystyrene-co-maleic Anhydride Blends Compatibility: A mesoscopic, Ewald Approach and Experimental Comparison

John Michael Tesha (✉ jcollinstesha@hotmail.com)

Tiangong University

Research Article

Keywords: Blend-module simulation, Polysulfone, Poly (Styrene-co-maleic Anhydride), DSC analysis, Phase Diagram, Energy of mixing

Posted Date: December 10th, 2021

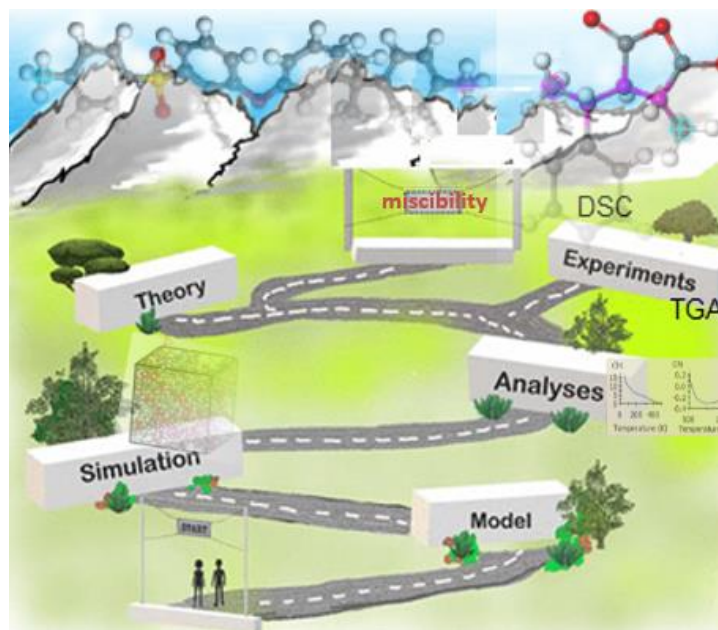
DOI: <https://doi.org/10.21203/rs.3.rs-1109742/v1>

License:  This work is licensed under a Creative Commons Attribution 4.0 International License.

[Read Full License](#)

23 **Graphical Abstract:**

24



25

26

27 **Highlights**

28 ➤ Amorphous cells built to perform MD simulations NVT-300 ps protocol at
29 various blending ratios

30 ➤ Schneier theory and thermodynamics study shows that PSF and PSMA is
31 thermodynamically compatible

32 ➤ The simulation reveals the PSF/PSMA blend is miscible at T higher than 400 K

33 ➤ Based on the shift of T_g by DSC confirms good interaction between PSF and
34 PSMA

35

36

37 **Abstract:**

38 This work aims to use molecular modeling to envisage the compatibility of
39 Polysulfone (PSF) and Poly (styrene-co-maleic anhydride) (PSMA) polymers blend.
40 A blend-module was developed based on the molecular dynamics (MD) technique
41 compared to an experimental study. Molecular dynamics simulations were achieved
42 using the condensed phase-optimized molecular-potentials for atomistic simulation
43 studies (COMPASS) force field with atomic-based electrostatic. The PSF/PSMA
44 blend compatibility facets and thermodynamic Gibb's free energy across ranges of
45 PSF/PSMA blend compositions were calculated. In doing so, the Flory Huggins chi
46 interaction parameter of mixing (χ) and solubility parameters (δ) were computed from
47 298K and on increasing temperature to predict the miscibility of the polymers blend
48 in the amorphous cell model by atomistic simulations. It was found that the blend-
49 system is miscible using the interaction chi parameter of Florry Huggins at a
50 temperature above 400K. At higher time-step, mesoscopic simulations for PSF/PSMA
51 reached equilibrium and computed free energy. Mixing energy indicated the stability
52 of the PSF/PSMA polymer blend. The results of this work narrate to the Flory
53 Huggins theory enthalpy of mixing for binary blend polymers at 40 and 60 % PSMA.
54 Additionally, the kinetic phase of the miscibility/immiscibility of the PSF/PSMA
55 blend system's miscibility/immiscibility was examined using Differential Scanning
56 Calorimetry (DSC). The result confirms the good interaction between the two
57 polymers through the shift of glass transition temperature (Tg) values within
58 individual polymers Tg. It is crucial to investigate the miscibility of two different
59 polymers for a variety of polymer applications. The MD simulation provides a
60 powerful, accurate computational tool in the estimation of polymer compatibilities.

61

62 **Keyword:** Blend-module simulation; Polysulfone; Poly (Styrene-*co*-maleic
63 Anhydride); DSC analysis; Phase Diagram; Energy of mixing

64

65 **1 Introduction**

66 Different types of polymer blends have been studied to make new polymer material,
67 such as polymeric membranes, which depend on the polymer-polymer blending's
68 miscibility [1]. There is increasing attention to studying different polymers with their
69 numerous applications in recent years [2, 3]. Studies indicated that Molecular
70 Dynamics (MD) simulations are essential tools, which can avoid countless
71 experimental and human errors in predicting the miscibility or blend compatibility of
72 polymers. [4, 5] [6-8].. In conjunction with MD simulations, Flory-Huggins theory
73 allows the easy way to study the compatibility of the blend polymers. MD simulations
74 have complex systems type simulations that enable the interactions between bonded
75 and non-bonded atoms for the built correct polymers [9, 10]. The interactions can be
76 combined in forcefield files in Material Studio. The simulations can be run using
77 Condensed-phase Optimized Molecular Potentials for atomistic simulations studies
78 (COMPASS), the techniques confirmed by various researchers [6, 11-13]. The
79 simulation systems are very sensitive to parameters set in the forcefield environment.
80 Among the properties of polymers, the interaction parameters can be estimated from
81 numerical paths of the blend polymers, which contain monomers' statistical structure
82 properties to mimic the polymers' behavior [14, 15].

83 Herein Polysulfone (PSF) common known polymer and has been studied extensively
84 in membrane applications due to its stability and potential in growing membrane
85 technologies. It has been broadly applicable in the area such as ultrafiltration,
86 microfiltration, and its surface modification for nanofiltration and reverses osmosis
87 for water treatment [16]. The modification of PSF can be done by blending with other
88 polymers. However, it is essential to be aware of compatibility or incompatibility to
89 achieve successful blending [17-19]. Poly(styrene-co-maleic anhydride) (PSMA)

90 versatile copolymer used membrane technology through blending with other polymers
91 to achieve attractive membranes with desirable features such as antifouling,
92 hydrophilicity, and heavy metals rejection and compatibility of PSMA and with
93 polymers has the great technological and scientific interest to researchers to achieve
94 successful fabrication of membranes [20-22].

95 This study aims to predict the compatibility/incompatibility of the PSF and PSMA by
96 molecular dynamics simulations - forcite blending tool in material studio 2017
97 software, and comparison with experiments such as thermal properties of these
98 polymers (Differential Scanning Calorimetry (DSC) and thermostability
99 thermogravimetric analysis – (TGA)). Furthermore, this present study reports the MD
100 simulation results obtained from the Discover Amorphous cell module of the material
101 studio 2017. The results obtained using simulations in conjunction with Flory-
102 Huggins theory allows us to foretell the phase behavior of PSF/PSMA blending at
103 various compositions. Thermodynamics analysis and using Schneier's approach of the
104 equation were as well employed to envisage thermodynamic compatibility.

105

106 **2. Theoretical relations**

107 MD simulations were done with the commercial software Material Studio (2017)
108 from Accelrys Inc. San Diego, CA, USA. The molecular mechanics and dynamics
109 simulation in the discover module and building of amorphous cells were done in this
110 work. The geometric optimization and potential energy estimations of arbitrary
111 periodic and molecular systems using classical mechanics were done with the forcite
112 module's help. Optimization is done to achieve the most stable structural
113 configuration. This optimization is conducted in two-steps in the system,
114 conformation adjustment and energy evaluations.

115 The blend-module using Dreiding [23] forcefield was performed in this work. The
116 “Dreiding” forcefield exemplifies intermolecular and intramolecular interaction
117 between polymers. The amorphous cell construction module was done in this work
118 with simulations giving the ability to study molecular systems and poly material type
119 by predicting the model's critical properties. This algorithm is suitable for building
120 longer chains and molecules in two separate steps, first creating an initial guess
121 structure and second structural relaxation to the minimum potential energy state [24,
122 25]. In this study, Condensed-phase Optimized Molecular Potentials for Atomistic
123 Simulation Studies (COMPASS) forcefield was employed since it allows accurate
124 prediction of the molecules' properties in the broad range, such as conformation,
125 structural vibrational, and thermos-physical properties. These properties are in
126 isolated condensed-phases in a wide range of conditions of pressure and temperature.
127 This is a consistent polymer forcefield (PCFF) used in modeling and simulation for
128 atomistic interaction, and the potential energy total of the system, is the result of the
129 sum of non-bond, bond (valence) and cross term interaction energies as shown in **Eq.**
130 **(1)**

131

$$132 \quad E_{TOT} = E_{valence} + E_{crossterm} + E_{non-bond} \quad (1)$$

133 The valence interactions energy ($E_{valence}$) consists of energies of the bond stretching
134 (E_{Bond}), valence angle bending energy (E_{Angle}), dihedral angle torsion energy ($E_{torsion}$),
135 and out of plane energy interaction or energy inversion (E_{oop} or $E_{inversion}$). Modern
136 COMPASS forcefield has a new denomination known as Urey Bradley (E_{UB}) that
137 takes into account the interaction between pairs of atom in 1 to 3 configurations that is
138 atom bonded to a common atom. **Eq. (2)** used in the system to obtain $E_{valence}$.

$$139 \quad E_{valence} = E_{Bond} + E_{torsion} + E_{Angle} + E_{oop} + E_{UB} \quad (2)$$

140 The forcefield's accuracy is done by introducing the correction factor as a bond or
141 angle distortion caused to the nearby atom. This is determined in cross-term
142 interaction energy ($E_{crossterm}$). This term gives out the dynamic properties of the
143 molecule through vibration frequencies, and later the interaction energy between non
144 bonded atoms ($E_{non-bond}$) consists of the energy of Van der Waals (E_{vdw}), coulomb
145 energy electrostatic ($E_{coulomb}$), and energy of Hydrogen bond (E_{H-bond}) shown in **Eq. (3)**

$$146 \quad E_{non-bond} = E_{H-Bond} + E_{Coulomb} + E_{vdw} \quad (3)$$

147 In COMPASS, Van der Waals's energy (E_{vdw}) is defined by the electrostatic and
148 potential energy from partial atom charges in a system calculated by the charge
149 equilibration method [26]. The electrostatic interaction was estimated by the Ewald
150 summation method, which is highly accurate in the estimation of long-range
151 molecular interaction [27]. The geometric optimization was done on each polymer
152 PSF, and PSMA and the forcite module were used for this optimization at 5000 steps
153 of energy minimization. The tolerance convergence for force and energy is 0.005
154 kcal/mol 1×10^{-4} kcal/mol, respectively.

155 **2.1. Blends tool calculation and simulation**

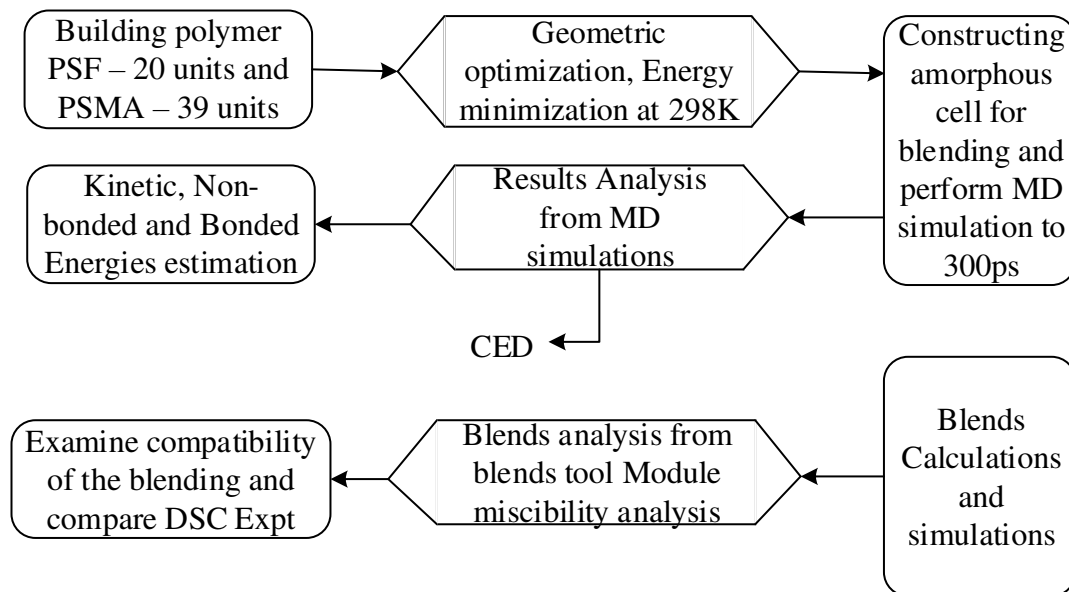
156 **2.1.1 Parameters to predict the miscibility**

157 The strength between molecules of the polymer materials is defined by the solubility
158 parameter (The Hilderbrand) – δ [28], which results in blending miscibility. This
159 parameter is calculated by the square root of cohesive energy density (CED), as
160 shown in **Eq. (4)**

$$161 \qquad \qquad \qquad \delta = \sqrt{\text{CED}} \qquad \qquad \qquad (4)$$

162 The important aspect of the simulation is the polymer molecular weight. Selecting the
163 length of a polymer chain in individual PSF and PSMA polymers, MD simulation was
164 used by performing dynamics to estimate δ . The stable value of δ is obtained at
165 sufficient individual monomers repeating units for running the simulation [29].

166 In this study, atactic PSF of 20 repeating unit monomer (**Fig. 2**) and isotactic alternate
167 copolymer PSMA of 39 repeating unit monomer (**Fig. 2**) used to construct the
168 amorphous cell weight fraction ratio 1:1 of the blend. Varying the repeating units
169 from 20-80 allows us to build the cell at different weight fraction ratios for the blend.
170 The polymers' densities were employed from the literature study [30], where PSF
171 density set 1.24 g/cm^3 and PSMA density set as 1.08 g/cm^3 , and such a system gives
172 out 945 atoms to be investigated for 1:1 polymer repeat unit blend. **Fig. 1** shows the
173 schematic procedure of simulation used to develop the polymer blends and
174 interactions that illustrate the methodology.



175
176
177

Fig. 1: Schematic procedure for simulation to develop the structure for polymer blends

178 Polymer molecular weight does not vary with cohesive energy density (CED).
179 However, it is highly related to the interaction of the polymer, and by neglecting
180 intramolecular forces, CED increases with energy (E_{coh}) per mole (V) of the polymer
181 shown in **Eq. (5)**. The solubility parameter values are shown in **Table 1**, comparing
182 literature and calculated from the forcite tool – CED.

183
$$\therefore CED = \frac{E_{coh}}{V} \quad (5)$$

184 It was reported that the CED depends on conversion degree and temperature to
185 achieve the solubility parameter. This shows that there is a linear relationship between
186 crosslinking density and CED. Therefore, the increase in temperature results in a
187 decrease in the solubility parameter, and the temperature has many effects with a
188 polymer having a lesser conversion degree [31].

189 Thermoset polymer with a higher conversion degree has a lower cohesive energy
190 density and solubility parameter. The cohesive energy density shows a linearly
191 decreasing relationship with the crosslink density. These properties also decrease
192 with increasing temperature and in thermoset polymers with lower conversion degrees
193 show a more significant temperature effect.

194

Table 1: Solubility parameters and other properties of the polymer

Polymer	Repeating Unit	Molecular weight repeating unit (g/mol)	Density (g/cm ³)	Solubility parameter (cal/cm ³) ^{0.5}	
				COMPASS (Charge Eq.)	Experimental
PSF ^a	20	442.5	1.238	8.27	9.92 [30]
PSMA ^b	39	202.1	1.079	8.01	9.4 [32]

195

Different researchers have reported other value solubility parameters from the PSF

196

experiment [33-35] and PSMA [36-39]. For this reason, it is important to take into

197

consideration the accurate method of using MD simulation for obtaining interaction

198

between these polymer blends depending on their CED. The blend-module in

199

simulation in predicting miscibility has a superior unique high efficiency taking into

200

account the Flory-Huggins interaction parameter (χ) across a range of temperatures

201

and ideal conditions. This method can envisage the thermodynamics of mixing

202

directly from two polymers' chemical structures (PSF and PSMA). It requires the

203

input of these structures into the blends simulation. This type of simulations'

204

uniqueness depends on combining the modified Flory-Huggins modeling [40-42] with

205

the MD simulation system [43].

206

The CED computation can enable us to obtain the energy of mixing (ΔE_{mix}) since the

207

Flory-Huggins model of this binary system is based on the thermodynamics of mixing

208

of the polymer/polymer system.

209

Generally, the energy of mixing is expressed, as shown in **Eq. (6)**

210

$$\Delta E_{mix} = \Phi_a \left(\frac{E_{coh}}{V} \right)_a + \Phi_b \left(\frac{E_{coh}}{V} \right)_b - \left(\frac{E_{coh}}{V} \right)_{mix} \quad (6)$$

211

The terms that are in brackets represent cohesive energies of individual pure polymers

212

(a, b) and the polymer blend (mix). However, Φ_a and Φ_b are volume fractions of each

213

polymer in the blending system. The equation

$$\Delta E_{mix} = \Phi_a \left(\frac{E_{coh}}{V} \right)_a + \Phi_b \left(\frac{E_{coh}}{V} \right)_b - \left(\frac{E_{coh}}{V} \right)_{mix} \quad (6) \text{ can also be}$$

expressed in terms of free energy mixing, as shown in **Eq. (7)**

$$\frac{\Delta G}{RT} = \frac{\Phi_a}{n_a} \ln \Phi_a + \frac{\Phi_b}{n_b} \ln \Phi_b + \chi \Phi_a \Phi_b \quad (7)$$

Whereby ΔG is the free energy of mixing (per mole), T is the reference absolute temperature of the simulation (in Kelvin), R is the molar gas constant, and χ is the Flory-Huggins interaction parameter. The beginning two terms in equation **Eq. (7)** are called combinatorial entropy, this is always negative, thus favoring a mixing state in the pure polymers. Finally, in the last term, the interaction parameter (Flory-Huggins) can be expressed according to case F.H [44], as shown in **Eq. (8)**. When the parameter is positive, the combinatorial entropy disfavors the polymer blend's mixing state and balances these two terms in **Eq. (7)**, resulting in different phase diagrams.

$$\chi = \left(\frac{\Delta E_{mix}}{RT \Phi_a \Phi_b} \right) V \quad (8)$$

Generally, this interaction parameter is essential in indicating the polymer miscibility, and it obeys the critical value, as shown in **Eq. (9)**.

$$(\chi_{ab})_{critical} = \frac{1}{2} \left(\frac{1}{\sqrt{m_a}} + \frac{1}{\sqrt{m_b}} \right)^2 \quad (9)$$

Whereby m_b and m_a are the degrees of polymerization of individual pure polymer. Therefore, when the blend system's interaction parameter is lower than the $(\chi_{ab})_{critical}$, then the system is miscible for the whole polymer composition range. Likewise, if the blend system's interaction parameter is slightly higher than the critical value, then the system exhibits the partial miscibility of the polymer blend. Besides, the two phases can exist, containing both compositions. Therefore, for significantly higher interaction

235 parameter values (χ) than critical, the system becomes completely immiscible. By
236 comparing the values of (χ) estimated from the equation **Eq. (9)** with the atomistic
237 simulation, the compatibility or miscibility behavior of the polymer blends can be
238 predicted [45, 46]. The traditional Flory-Huggins modeling, each component in the
239 blend system, has the lattice site with coordination number Z in which the energy
240 mixing is given by equation **Eq. (10)**

$$241 \quad \Delta E_{mix} = \frac{1}{2} Z (E_{sb} + E_{bs} - E_{bb} - E_{ss}) \quad (10)$$

242 E_{bb} is the binding energy base-base pair, E_{bs} is a binding energy base-screen pair, E_{sb}
243 is the binding energy screen-base pair, and E_{ss} is the binding energy screen-screen
244 pair. These are energies of interaction between two polymers and, together with the
245 interaction parameter (χ), can generate energy mixing.

246 The blends-button is selected from the menu toolbar and then the menu's dropdown to
247 select calculation from the module dropdown list. In the setup input section tab, the
248 empty row under the molecule must be assigned to input the structures that have been
249 geometrically optimized by forcite. In the Blends dialogue calculation setup, the quality
250 accuracy has been changed from medium to fine, corresponds to a bin width of 0.2
251 kcal/mol to 0.02 kcal/mol, respectively. After that, it uses the same dialogue (Blends
252 Calculation) energy tab selected for setup. The forcefield was set to Dreiding and changed
253 the charges to the 'charge using 'QEq' to calculate the Flory-Huggins interactions.
254 Finally, the Run option was selected in the blends calculation dialogue to achieve the
255 polymer's mixing. During the blending simulation, the new file of the PSF mixture was
256 created in Project Explorer. After the simulation was completed, the Blend-Module
257 analysis was selected from the menu bar. The analysis dialogue in the blend-module
258 allows us to examine the interaction parameter (χ), the energy mixing, and the phase

259 diagrams. This blend-module system was validated by its calculations done in the Material
260 studio [47, 48].

261 **2.1.2 Experimental solubility parameters**

262 **2.1.2.1 Schneier theory and Thermodynamics analysis**

263 The enthalpy of mixing Δm reported from Schneier's theory equation **Eq. (11)** can
264 also determine the compatibility of the polymers using experimental parameters from
265 different literature and depending on the density of each polymer ρ_a , and ρ_b the
266 solubility parameter of each polymer δ_a , and δ_b the molecular weight of each
267 polymer M_a and M_b and weight fraction for each polymer W_a and W_b . The subscript
268 components "a" and "b" represent two polymers blend, and for this report,
269 specifically, "a" is PSF, and "b" is PSMA. The Schneier equation below is used to
270 obtain the enthalpy of mixing for blended polymers, of which from the calculations, it
271 was reported by Flory-Huggin's theory that for the composite polymers to be
272 compatible, the enthalpy of mixing $\Delta m < 0.01$ cal/mol likely for incompatible
273 polymer blend the enthalpy of mixing $\Delta m > 0.01$ cal/mol.

$$274 \quad \Delta H_m = \left\{ W_a M_a \rho_a (\delta_a - \delta_b)^2 \left[\frac{W_b}{(1-W_b) M_b \rho_b + (1-W_a) M_a \rho_a} \right]^2 \right\}^{\frac{1}{2}} \quad (11)$$

275 In order to obtain the status of thermodynamics compatibility, the Gibbs free energy
276 ΔG_{mix} of blended polymer can be used to determine the thermodynamics
277 compatibility state. Gibbs free energy ΔG_{mix} is dependent on the enthalpy of mixing
278 ΔH_m of the mixed polymers calculated from the above equation, Entropy of mixing
279 ΔS_{mix} , and temperature of mixing T (K) at which mixed polymers become miscible
280 [49]. Different researchers have reported that Gibbs's free energy increase with the
281 increase in compatibility degree. Therefore, the thermodynamics equation **Eq. (12)** is

282 used to calculate the Gibbs free energy of mixing, and according to the
283 thermodynamics theory [50] for thermodynamic compatible polymers blend, the
284 Gibbs free energy $\Delta G_{mix} < 0$ cal/mol and thermodynamic incompatible $\Delta G_{mix} > 0$
285 cal/mol.

$$286 \quad \Delta G_{mix} = \Delta H_m - T\Delta S_{mix} \quad (12)$$

287

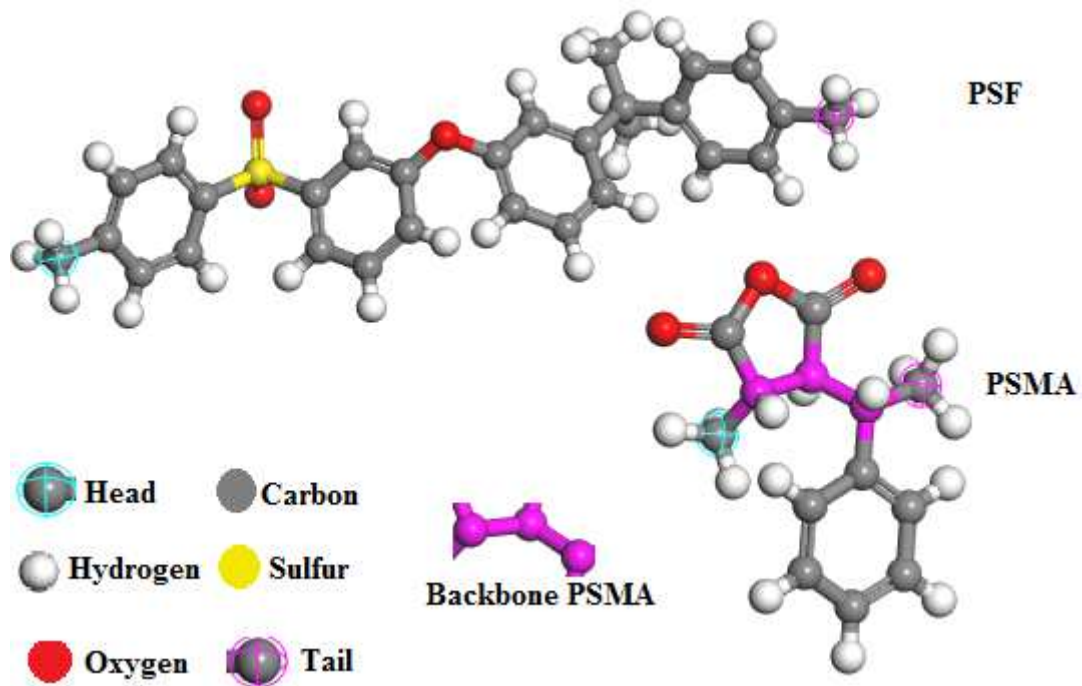
288

289 **3 Experimental section**

290 **3.1. Materials**

291 Polysulfone (PSF) molecular weight about 97,000 g/mole with repeating unit
292 molecular weight 442.52 g/mole. It was purchased from Dalian Polysulfone Plastic
293 Company Ltd (Liaoning province China), Crystal-clear powder form PSMA-5
294 molecular weight about (1.2×10^5) g/mole, MA = 26% wt was purchased from Solvay
295 solexis (Belgium).

296 **Fig. 2** shows the monomers' chemical structure (PSF and PSMA) used in this study.



297

298 **Fig. 2: Chemical structure for PSF and PSMA monomers**

299

300

301

302

303

304

305

306 **3.2. Thermal Properties Analysis**

307 **Table 2** indicates the denomination to describe the samples used in this study for
308 thermal properties. The polymer miscibility criterion is to obtain a single glass
309 transition temperature (T_g) in a polymer blend. This is the result of the miscibility at
310 the molecular level of the polymer blends. Additionally, the single T_g can indicate the
311 homogeneity of the polymer chain's distribution in polymer films [51].

312
313

Table 2: Description of the samples-polymer concentrations

Name	PSF (% wt)	PSMA (% wt)
T0	100	0
T1	80	20
T2	60	40
T3	40	60
T4	20	80
T5	0	100

314

315 **3.2.1 Differential Scanning calorimetry (DSC) investigation**

316 The glass transition temperature (T_g) values of pure polymers and polymer blend
317 samples were studied by NETZSCH DSC 200F3 Maia-Germany model instrument to
318 examine the polymer blend and rigidity's miscibility of the polymers. Samples were
319 measured at an average of 8-12 mg, and the thermal scanning was conducted from
320 20 °C to 220 °C at a heating rate of 10 °C/min under the flow of nitrogen (N_2).

321 **3.2.2 Thermogravimetric Analysis (TGA)**

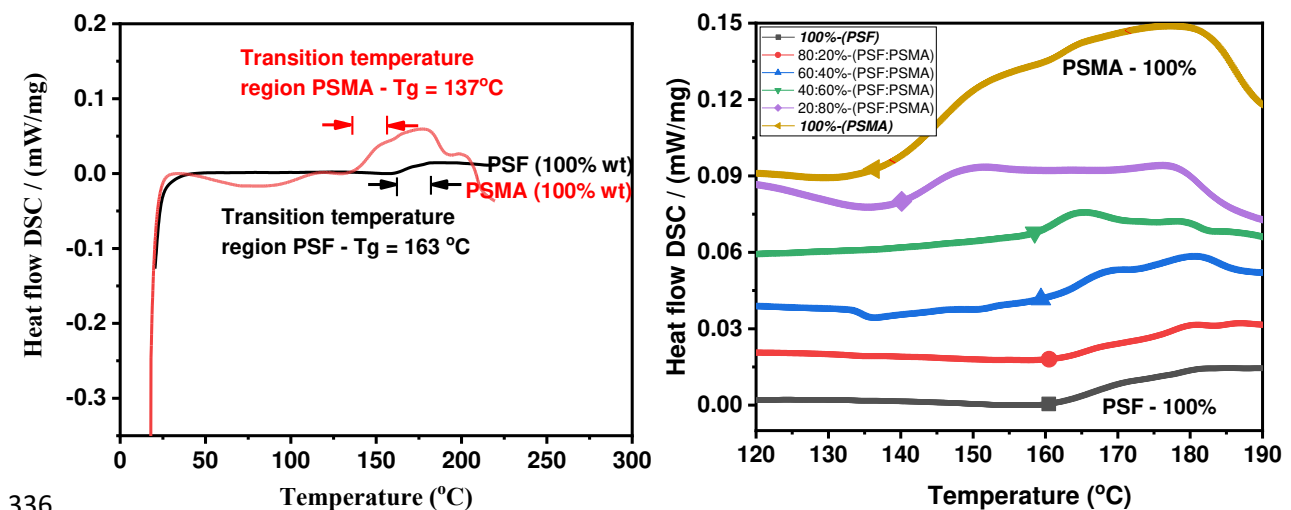
322 NETZSCH STA449-F3-Jupiter instrument was used to analyze the thermal stability
323 of the polymers. Samples at different polymer concentrations were weighed at an
324 average of 17-19 mg and transferred to Alumina ceramic crucible for thermal analysis.
325 Crucibles are non-reusable with high-temperature stability, a wide range of operating

326 temperature, and the maximum working temperature for these crucibles is 1750 °C
327 [52]. TGA study was done from 40 °C to 800 °C at a constant heating rate of
328 20 °C/min, and nitrogen gas was used at a flow rate of 1/ (ml/min):50.

329 4. Results and Discussion

330 4.1 DSC Results of PSF/PSMA

331 One of the most typical experimental methods to evaluate the polymer-polymer
332 compatibility is by determining the polymer blend's T_g value and comparing it with
333 an individual pure polymer (PSF and PSMA). This method can experimentally study
334 the compatibility between the PSF and PSMA polymer. **Fig. 3** shows the results of the
335 DSC for the PSF/PSMA.



337 **Fig. 3: DSC spectra of PSF/PSMA blending at various concentrations ratio**

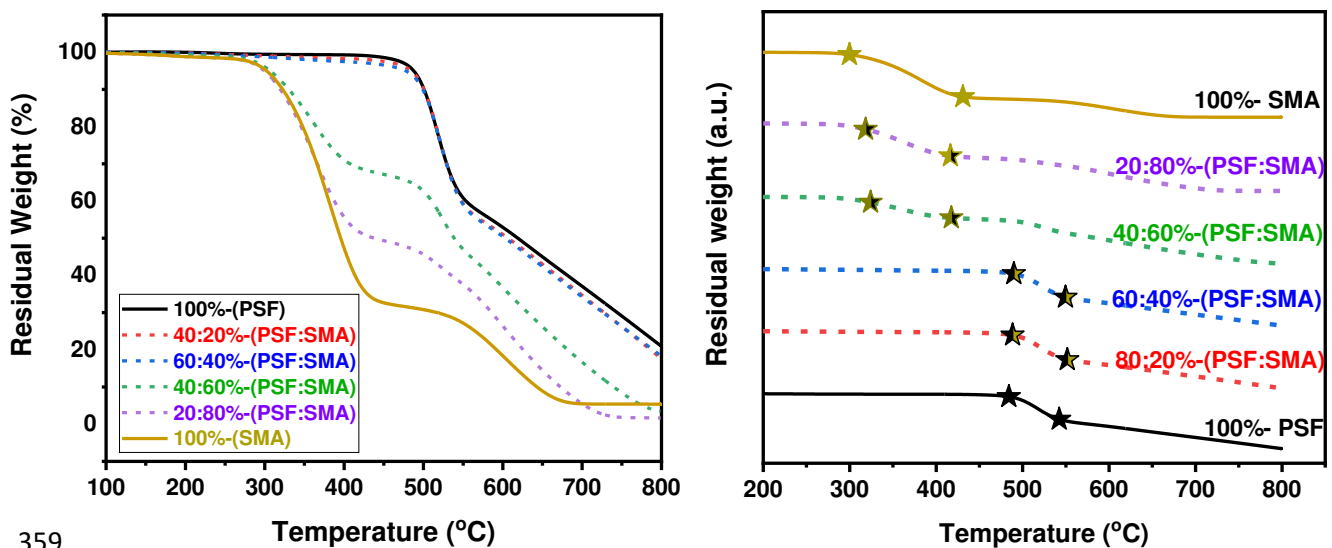
338 The criteria behind the polymer miscibility are obtaining the single value of T_g in a
339 polymer blend system, which indicates the miscibility at the molecular state [51].
340 From **Fig. 3** it is showing that the T_g of individual polymers is different. That is, pure
341 PSF has a T_g of 163 °C, which is higher than pure PSMA having T_g of 137 °C.
342 However, varying polymer concentration of polymer as indicated in **Table 2**, the T_g
343 values change and different from that pure PSF and pure PSMA. These differences

344 can be due to many van der Waals interactions between two polymers that lose the
345 identity [53].

346 Furthermore, there is a modeling interaction as the blend's distinct T_g values are in
347 between those of individual polymers (PSF and PSMA). As an increase in the PSF
348 polymer fraction in the blending, T_g's value increases uniformly due to the higher T_g
349 of PSF. The miscibility is observed below 50% of PSMA as it is seen from **Fig. 3** that
350 a single gradual increase of T_g values approaches a similar value to that of PSF.
351 However, above 50 % PSMA, the blend T_g is seen to shift closer to pure PSMA and
352 become immiscible. These results suggest further analysis by MD simulation to
353 understand and compare the miscibility at the edge boundary to avoid overestimations
354 and obtain the equilibrium polymer-polymer interaction and miscibility boundary
355 [54].

356 4.2 Thermogravimetric Analysis (TGA)

357 The thermal analysis for the PSF/PSMA data collected from the TGA instrument is
358 indicated in **Fig. 4**.



359

360

Fig. 4: TGA Analysis of the PSF/PSMA polymer blend

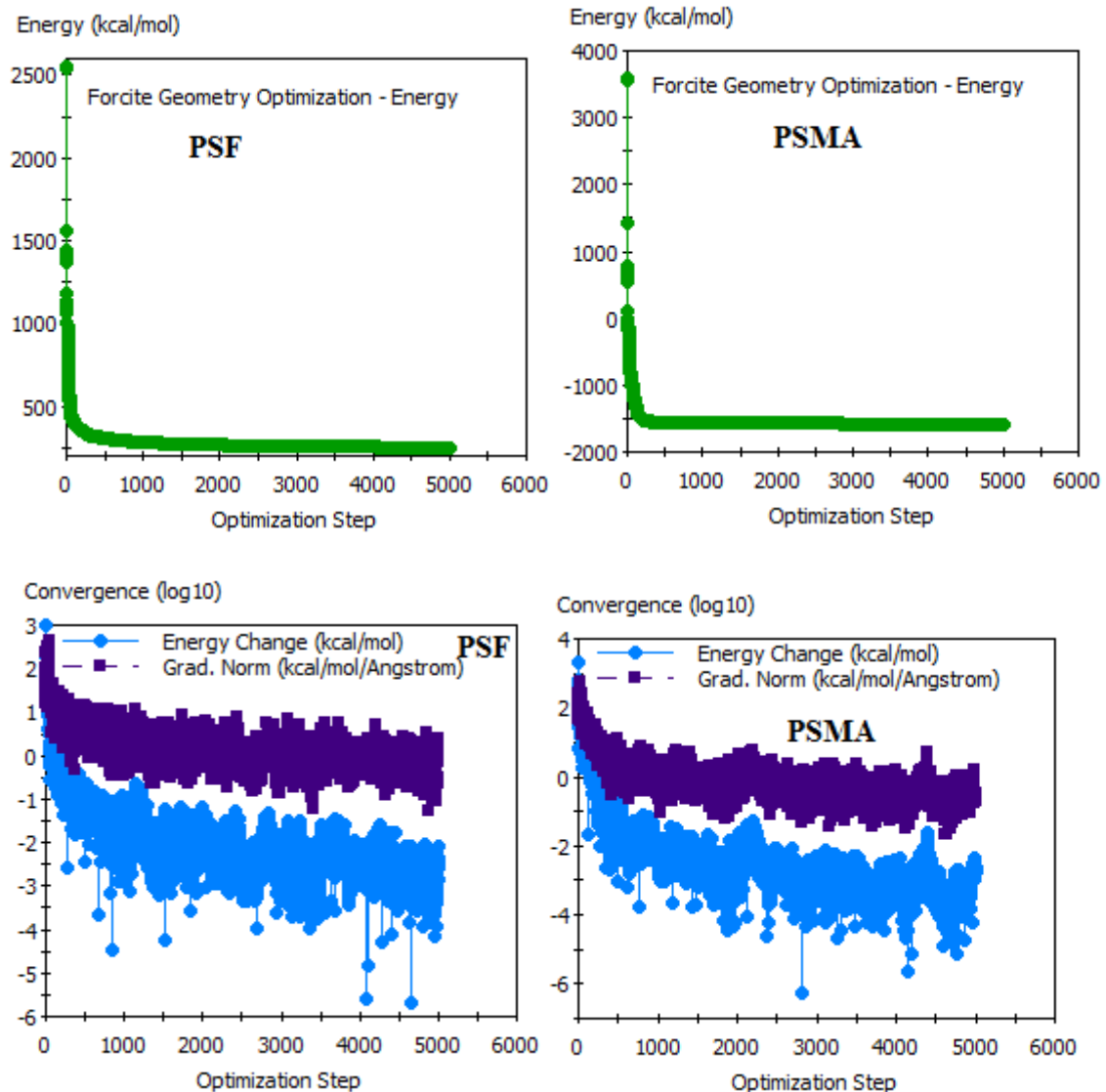
361 For pure PSF, the degradation onset temperature is seen at **484.9 °C**, and thermal
362 degradation continued up to a temperature of **542.9 °C**. Conversely, pure PSMA is
363 seen to have a degradation onset temperature at **301.8 °C**, and the final degradation
364 temperature was found to be **428.8 °C**. This is attributed to the chemistry nature of the
365 two polymer structures, where cleavage of C=C in benzene (aromatic) ring in PSF
366 will be last, and C-O in maleic anhydride cleaved more easily compared to C=C of
367 PSF [55, 56]. The degradation behavior between pure PSF and pure PSMA continued
368 to be seen (PSF/PSMA-polymer blend). The blending of PSMA in the PSF matrix
369 improved thermal stability at a low concentration of PSMA up to 40% of the polymer
370 blend. The stability from 60:40% (PSF:PSMA) blend up to 100% pristine PSF was
371 found to have an onset degradation temperature of **484.9 °C** and a final degradation
372 temperature of **550.8 °C**. This is attributed to the significant part of the blend
373 occupied by highly thermally stable pristine PSF.

374 Additionally, a further increase of PSMA (20:80%-PSF:PSMA) lowers the thermal
375 stability, and degradation onset temperature was observed to decrease to **316.8 °C**,
376 and final degradation temperature was found to be **414.5 °C**. It is evidently confirmed
377 that the two polymers' interaction at a low concentration of PSMA shows good
378 agreement. As indicated in **Fig. 4**, a single degradation peak in the TGA graph. This
379 confirms the PSF/PSMA blend's miscibility is in the range of 0 to 40% PSMA, as
380 seen in the uniform behavior between the two pure polymers.

381 **4.3 MD Simulations**

382 Structure built in the Material Studio before running simulations was optimized at
383 5000 steps. **Fig. 5** is shown that profiles were generated during the optimization of
384 these structures. The optimization aims to bring the structures' stable configuration,
385 conformation, and minimal energy evaluation to be used for constructing amorphous
386 cell and blending simulation. It is seen that PSF structure energy was minimized from

387 2553.4 kcal/mol to 250.3 kcal/mol, whereas for PSMA structure, the energy was
 388 reduced from 3603 kcal/mol to -1578 kcal/mol using the conjugate gradient method.
 389 This is also done in order to bring its excellent performance and reliability from the
 390 initial starting point [57].



391

392

393

394

Fig. 5: Energies minimization and convergence profiles generated during optimization

395

Amorphous cell construction and Dynamics analysis

396

Unit cells of three-dimensional cubic were constructed having conditions of the

397

periodic boundary in amorphous cell module, as seen in **Fig. 6**. The cells were

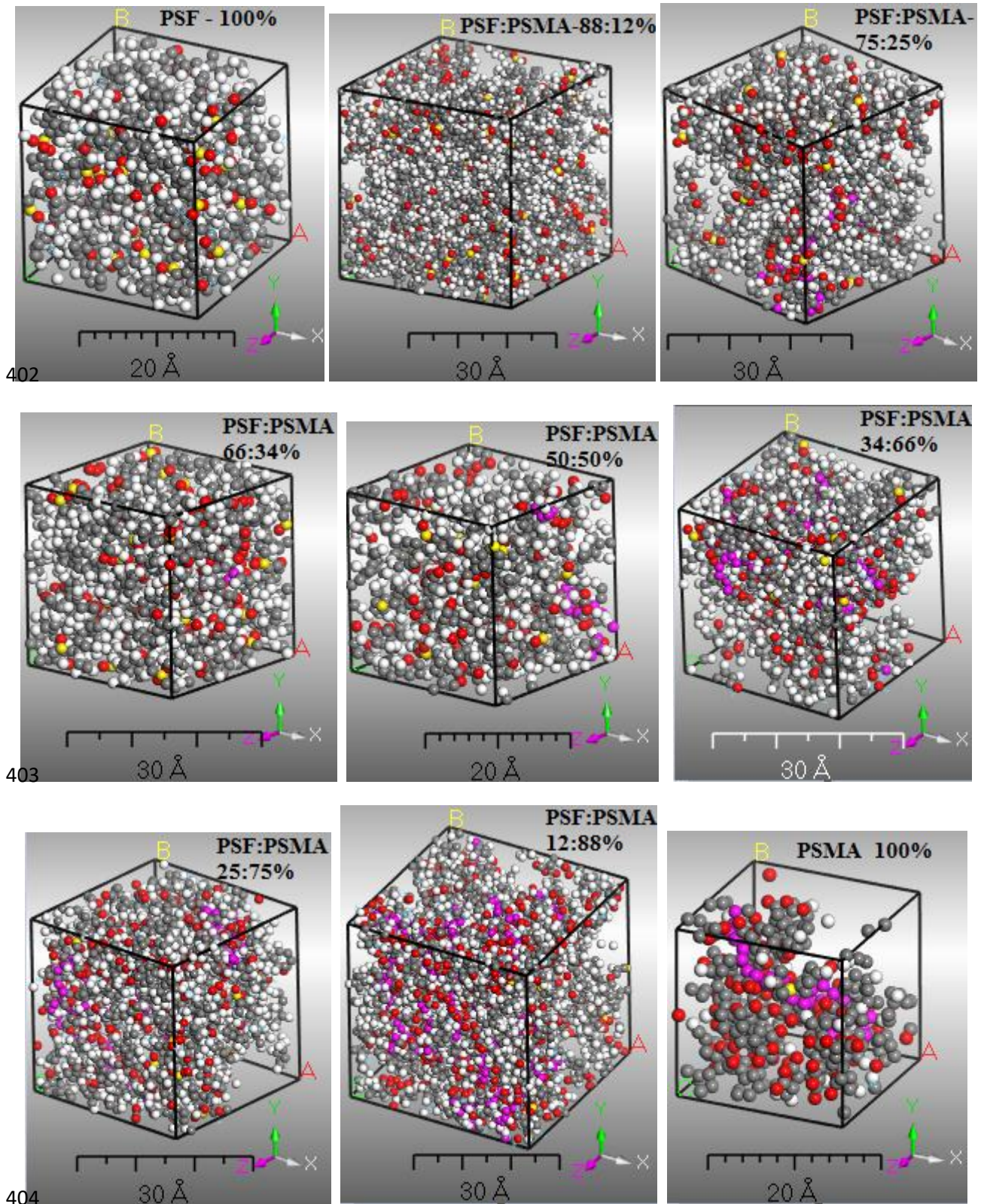
398

optimized to minimize energy before running MD simulations. The simulation runs at

399

300ps, and 298K with NVT ensemble means constant-volume/constant-pressure

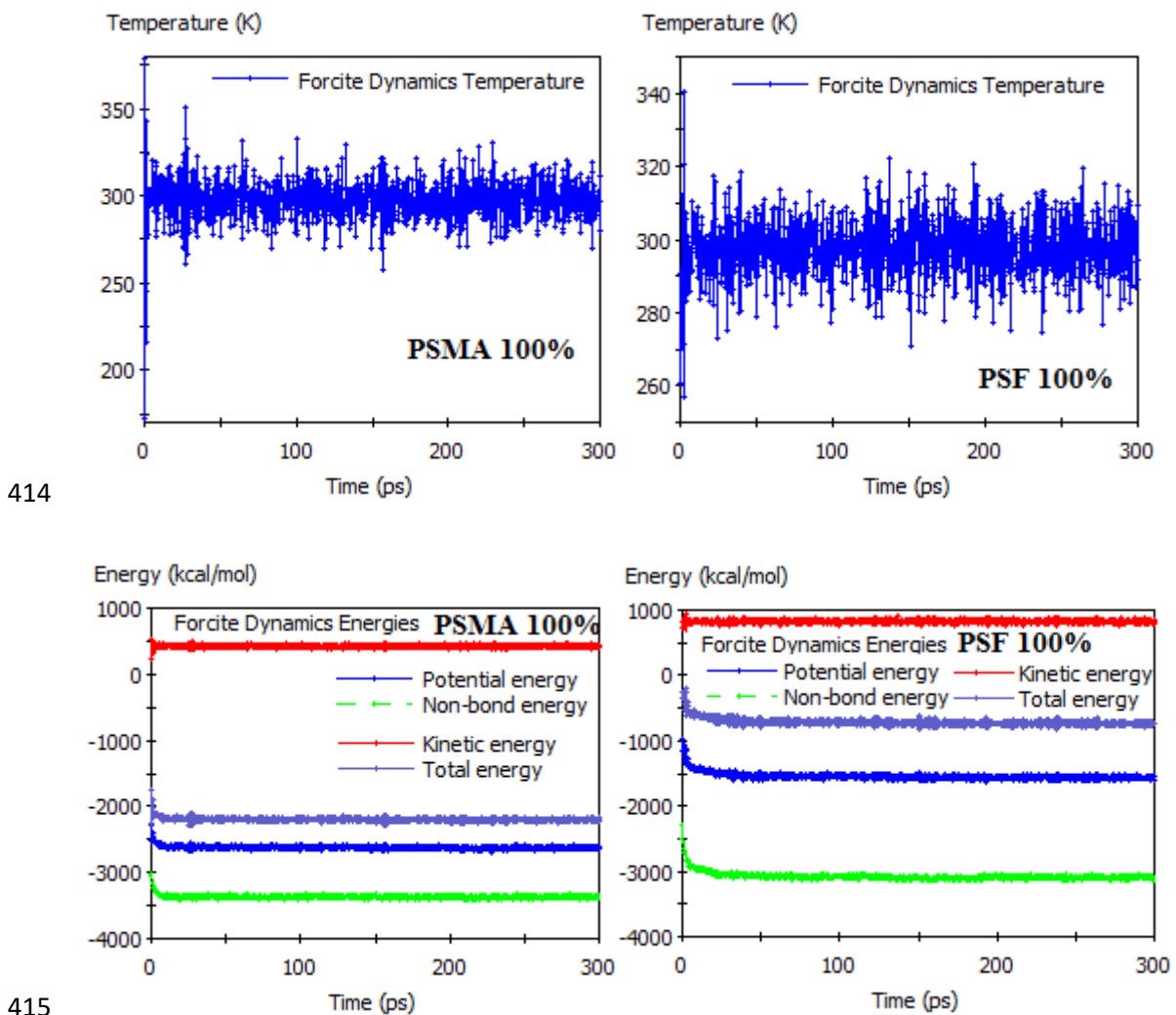
400 dynamics, this ensemble dynamics are set in such a way to allow the system to
401 exchange heat with the environment at the controllable temperature.



405 **Fig. 6: Simulated amorphous cells at various compositions of PSF and PSMA**

406

407 Here Carbon atoms are shown grey; Oxygen atom is shown red in color, Sulfur atoms
408 from PSF yellow in color, and Hydrogen are shown white. For model protocol,
409 different ratios number of chains are constructed in a unit cell. During MD simulation,
410 fluctuation profiles of temperature, non-bonded, potential, and total energies were
411 generated for each unit cell. **Fig. 7** shows an individual pure polymer PSF and PSMA
412 generated profiles (temperature and energies). Further studies on each cell are shown
413 in Supplementary Figure S1



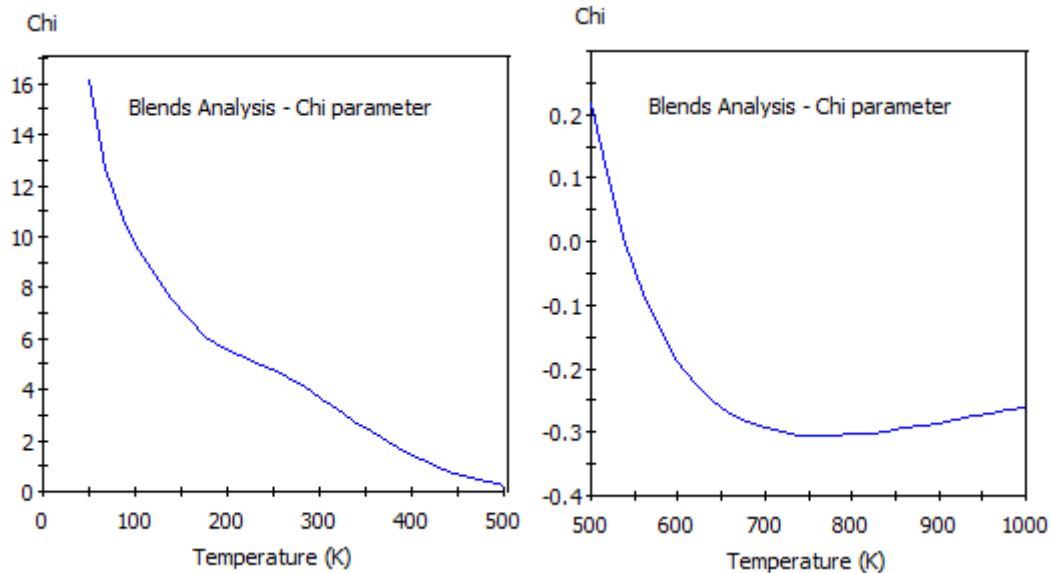
416 **Fig. 7: Fluctuation profiles of temperature, potential, non bonded, kinetic, and**
417 **total energy plot vs. MD simulation time in ps.**

418

419 The results show that, for the duration of 300 ps simulation time, there is no
420 significant change in the structures; hence, the time was adequate to attain the state of
421 equilibration protocol. Also, to circumvent the entrapment of the simulated systems in
422 a local metastable state of the minimized energy from geometric optimization, MD
423 simulations were run at NVT ensemble then followed by NPT (constant
424 pressure/content temperature dynamics) so to overcome the energy barrier between
425 the minimal high energy by thermal energy provided [6]. The projected density of
426 each amorphous cell is assumed from 1.24 g/cc to 1.08 g/cc from individual polymers.

427 **4.4 Flory–Huggins interaction parameter from blend-module analysis**

428 According to the theory of Flory-Huggins, when the interaction parameter (χ) is less
429 than one and up to negative values, two molecules at the particular temperature are
430 miscible, or interaction is favored. Furthermore, if χ is a positive value or higher than
431 one, it indicates that two molecules can not be easily mixed [40, 41]. Likewise, when
432 the interaction parameter value is substantial, the free energy overcomes the
433 combinatorial entropy of mixing, and the molecules will separate into two different
434 phases. This part aims to obtain the value of χ for our two polymers blend (PSF and
435 PSMA). However, the material studio software was capable of producing plots, as
436 indicated in *Fig. 8* from the Blend-module analysis dialogue at various temperatures
437 to predict miscibility. The χ value obtained at 298 K particular temperature was 5.014,
438 which confirm immiscible. However, from this result, it shows that the interaction
439 parameter changes continue to change on the increase in temperature where the
440 system becomes miscible from 400 K temperature, and above, at this particular
441 temperature (400 K), the Flory-Huggins interaction parameter was seen to shift to
442 lower values than 1 up to negative values.



443

444 **Fig. 8: Flory-Huggins interaction parameter (χ) as a function of temperature (K)**
 445 **for PSF and PSMA polymers blending**

446 Blends combines a modified Flory-Huggins model and molecular simulation
 447 techniques to calculate the compatibility of binary mixtures. Two important
 448 extensions to the Flory-Huggins model are employed:

449 Blends incorporates an explicit temperature dependence on the interaction parameter.
 450 This is accomplished by generating a large number of pair configurations and
 451 calculating the binding energies, followed by temperature averaging the results using
 452 the Boltzmann factor and calculating the temperature-dependent interaction
 453 parameter.

454 Blends is an off-lattice calculation, meaning that molecules are not arranged on a
 455 regular lattice as in the original Flory-Huggins theory. The coordination number is
 456 explicitly calculated for each of the possible molecular pairs using molecular
 457 simulations.

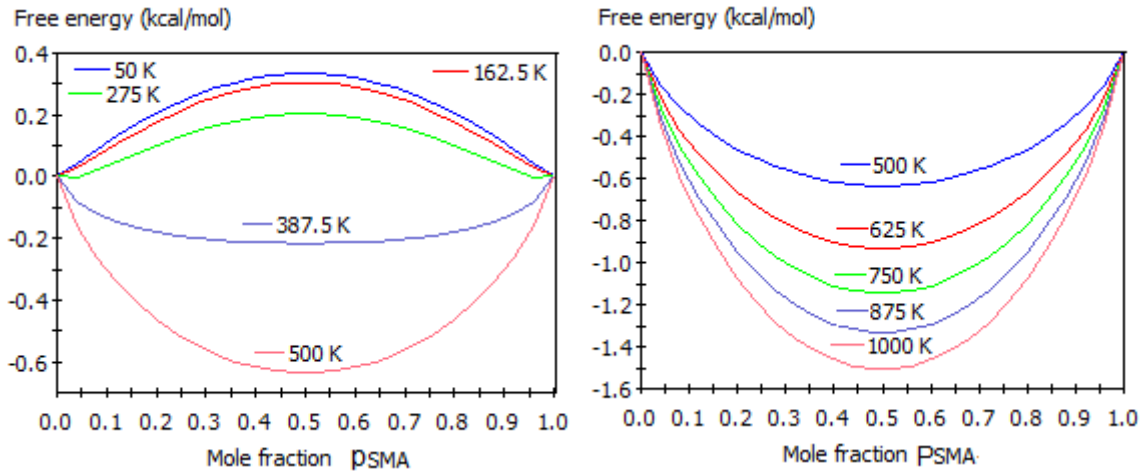
458 These two extensions to the classical Flory-Huggins theory of mixing are considered
 459 in the blend simulation.

460 Also, by substituting the temperature-dependent interaction parameter, χ , in the Flory-
461 Huggins expression, the free energy is known for all compositions and temperatures.
462 From this, the phase diagram of the mixture can then be determined by locating the
463 critical point, the coexisting curve (binodal), and the stability curve (spinodal) in the
464 two-phase diagram.

465 As with any molecular simulation, the results obtained depend on the accuracy of the
466 forcefield. Blends supports a wide variety of forcefields.

467 In the traditional Flory-Huggins model, each component occupies a lattice
468 site. Although it is possible to use a fixed lattice coordination number in Blends, in
469 calculating the interaction parameter χ , Blends also provides the option to calculate
470 the coordination numbers for each pair and considered when running blending
471 simulation

472 In addition to the interaction parameter, it is crucial to analyze the system's mixing
473 energy and free energy to observe the value close to zero, suggesting miscibility.
474 Figure S2 can be used to confirm further on miscibility study of PSF and PSMA. The
475 more decrease of energy mixing to less than zero (negative values) indicates PSF and
476 PSMA are miscible. The free energy plot at the various temperature as a function of
477 the mole fraction of PSMA was generated from the system's analysis. This plot is
478 presented in **Fig. 9**. This plot can be further analyzed using the enthalpy of mixing by
479 Schneier's theory (at 298K), which will be discussed later in this study. However, as
480 the temperature increases, it is free to shift to the negative side at the similar
481 composition of PSMA. This is attributed to the temperature-dependent miscibility
482 behavior, as confirmed earlier in this work.



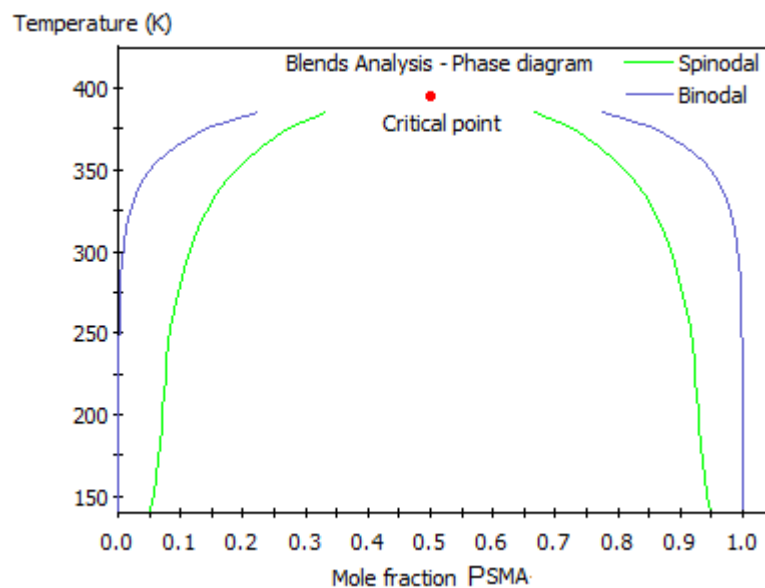
483

484

Fig. 9: Free Energy analysis function of mole fraction of PSMA

485 **4.5 Phase Diagram of the PSF/PSMA blend**

486 In illustrating the compatibility between polymers, phase diagrams are essential as
 487 they developed from the free energy of the binary system of blend [43, 58, 59]. This
 488 part aims from the phase diagram, where we obtain information about the temperature
 489 range of PSF/PSMA mixture for miscible and immiscible. An immiscible polymer
 490 mixture splits into two phases, wherein the phase diagram, and we can read its
 491 composition. **Fig. 10** is the phase diagram obtained from the blend-module analysis.



492

493

Fig. 10: Phase diagram for the binary system of PSF /PSMA

494 The pieces of information obtained from this plot, such as critical point (in red dot),
495 Binodal (Blue line color), and spinodal (Green line color). Furthermore, these results
496 show that at the critical point, there is a coexistence region for PSF / PSMA and the
497 PSF/PSMA blend by split into two phases, which results in lower free energy, as
498 illustrated earlier. The temperature at a critical point found was 400 K at a mole
499 fraction of 0.5 PSMA. This plot has a single critical point that confirms one
500 coexistence region. However, a complex binary system of polymer blend may have
501 more than one critical point in its phase diagram due to several coexistence regions.
502 Thus, the spinodal is linked to the coexistence region's separation into two phases,
503 whereas the binodal links with the coexistence region in this phase diagram. In the
504 region between the spinodal and binodal, the polymer blend system is metastable.
505 That is, the blend will separate only after sufficiently high fluctuation. The region in
506 the spinodal bounded up to lower temperatures the PSF/PSMA is immiscible, which
507 agrees from the earlier illustration of Flory Huggins interaction parameter and mixing
508 energy. Any fluctuation causes immiscibility as the system is unstable in the spinodal
509 region. Additionally, above the binodal region, PSF /PSMA blend system is miscible
510 and stable.

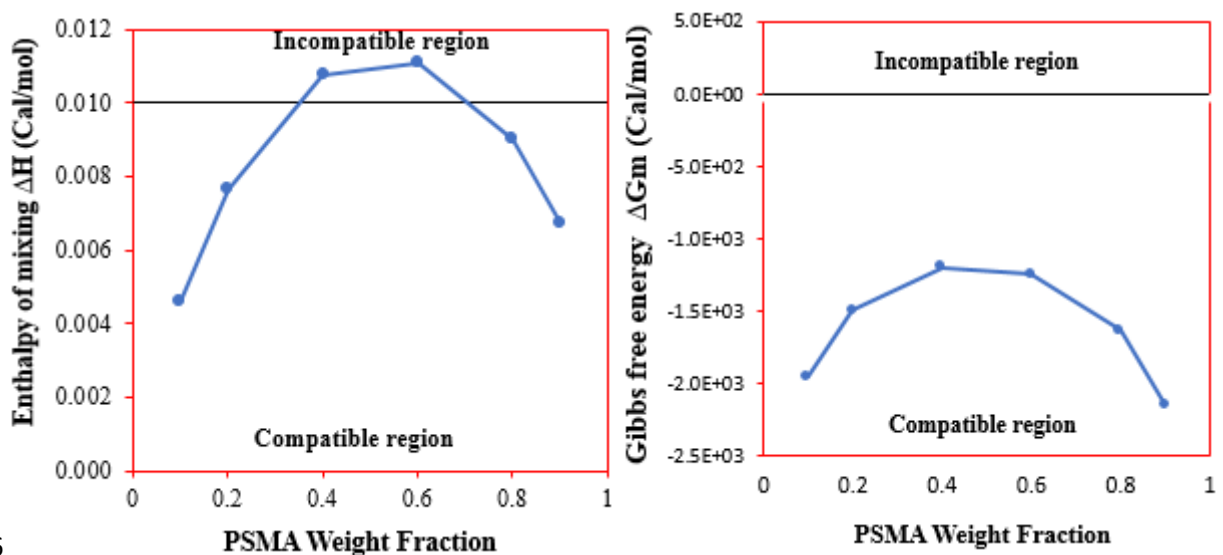
511 Recent advances in molecular simulation techniques have improved this situation.
512 Accurate forcefields can be obtained by defining parameters using structural and
513 spectral data. Molecular simulations can be performed on well-characterized systems,
514 leading to a better fundamental understanding of atomic-level interactions. This
515 information can then be used to predict useful physical properties of systems that are
516 less well characterized. Many factors govern mixing processes, including the
517 temperature and the chemical nature of the individual components. Additional factors
518 may be involved for polymers; for example, chain packing, the degree of crystallinity,
519 molecular weight, and chain flexibility. Not all of these factors can be addressed using

520 molecular simulation techniques. However, it is possible to obtain structural data for
521 the individual components in a mixture and to calculate the interaction energy terms
522 required for the thermodynamic expressions.

523

524 4.6 Compatibility by Schneier theory and thermodynamics

525 Solubility parameters from the experimental work together with densities and
526 molecular weight of the repeating units can be used to estimate enthalpy of mixing
527 using **Eq. 11**. Therefore, the enthalpy of mixing obtained using experimental data of
528 solubility parameters from **Table 2** can be plotted against the mole fraction of PSMA,
529 as indicated in **Fig. 11**. It is mentioned that the Schneier theory of compatibility is
530 assumed only at the temperature of the blend system 298 K, and interest lies in the
531 system of compatible solids at room temperature. Hence solubility parameters and
532 density used in the calculation were at 298K [60]. Therefore the result disagrees with
533 simulations; however, only at 40 % up to 60% PSMA blend agree with MD
534 simulation blends. Only 60% of PSMA agree with the DSC experiment, and below
535 40% PSMA as illustrated earlier in this study.



536

537 **Fig. 11: (a) PSF/PSMA Schneier calculation – Enthalpy of mixing (b) PSF/PSMA**
538 **Gibb's Free energy graph - thermodynamic theory of compatibility**

539

540 It is seen that the PSF/PSMA polymer blend is partially compatible. From 0.4 to 0.6
541 PSMA wt/wt, the enthalpy of mixing is higher than the limit of Flory Huggin's theory
542 (10^{-3} cal/mol), which changes to the incompatibility on increase further PSMA weight
543 fraction turn to the compatible state. Therefore, from the Schneier equation
544 calculation, the system is partially compatible, which allows further investigation,
545 such as MD Simulations, compared to the experimental DSC approach. In **Fig. 11**.
546 From these (**12**, it is seen that Gibb's free energy is dependent on the enthalpy of
547 mixing calculated from the Schneier equation, the entropy of mixing and temperature
548 at which polymer blend system, higher temperature > 298 K as higher than 400K the
549 system is thermodynamically compatible with an increase pf PSMA polymer
550 composition in the blend system.

551 **5. Conclusion**

552 In this study, the miscibility between PSF and PSMA was intensively examined by
553 MD simulation and the experiment. The energy mixing, Flory-Huggins interaction
554 parameters, amorphous cell, and phase diagrams were studied in this work. The
555 results showed that PSF and PSMA are miscible from a temperature above 400K with
556 an optimal weight fraction of PSMA of about 0.5. In the DSC experiment, the two
557 polymers show a good interaction as the shift of T_g values within the range of
558 individual polymer T_g . Furthermore, based on thermodynamics techniques,
559 experimental data together with MD simulation blending are verified; thus, two
560 polymers PSF/PSMA thermodynamically compatible. In this perspective, membranes
561 such as for water treatment and fabrication of these blends (PSF and PSMA) can be
562 done via thermally induced phase separation method with glycol derivative diluent to
563 dissolve the polymer blends at high temperature.

564

565 **Acknowledgment**

566 Authors gratefully acknowledge the Tianjin Science and Technology Planning Project
567 (Grant No. 18PTZWHZ00210), National Natural Science Foundation of China (Grant
568 No. 21576209 and 21878230), and Innovative Team in University of Ministry of
569 Education of China (Grant No. IRT-17R80) for their financial support. Also, I would
570 like to thank the School of Materials Science and Engineering, Tiangong University,
571 China, for their kind assistance.

572

573 *Declarations

574

575 Funding: (Authors gratefully acknowledge the Tianjin Science and Technology
576 Planning Project (Grant No. 18PTZWHZ00210), National Natural Science
577 Foundation of China (Grant No. 21576209 and 21878230), and Innovative Team in
578 University of Ministry of Education of China (Grant No. IRT-17R80)

579

580 Conflicts of interest/Competing interests: (No declared conflict of Interest)

581

582 Availability of data and material: (Not applicable)

583

584 Code availability: (Not applicable)

585

586 Authors' contributions: (Not applicable)

587

588

589 **References**

- 590 [1] H. Abdul Mannan, T.M. Yih, R. Nasir, H. Muhktar, D.F. Mohshim, Fabrication
591 and characterization of polyetherimide/polyvinyl acetate polymer blend
592 membranes for CO₂/CH₄ separation, *Polymer Engineering & Science* 59(S1)
593 (2019) E293-E301.
- 594 [2] M.R. Aguilar, J. San Román, *PSMArt polymers, and their applications*,
595 Woodhead publishing 2019.
- 596 [3] R.R. Luise, *Applications of High-Temperature Polymers: 0*, CRC Press 2018.
- 597 [4] S.S. Jawalkar, K.V. Raju, S.B. Halligudi, M. Sairam, T.M. Aminabhavi,
598 Molecular modeling simulations to predict the compatibility of poly (vinyl
599 alcohol) and chitosan blends: a comparison with experiments, *The Journal of*
600 *Physical Chemistry B* 111(10) (2007) 2431-2439.
- 601 [5] M. Linyu, W. Xigang, L. Yaqing, W. Junyuan, *Computer Simulation of PAN/PVP*
602 *Blends Compatibility and Preparation of Aligned PAN Porous Nanofibers via*
603 *Magnetic-Field-Assisted Electrospinning PAN/PVP Blends*, *Materials Science*
604 25(1) (2019) 54-59.
- 605 [6] J. Gupta, C. Nunes, S. Vyas, S. Jonnalagadda, *Prediction of solubility parameters*
606 *and miscibility of pharmaceutical compounds by molecular dynamics*
607 *simulations*, *The Journal of Physical Chemistry B* 115(9) (2011) 2014-2023.
- 608 [7] P. Barmpalexis, A. Karagianni, K. Katopodis, E. Vardaka, K. Kachrimanis,
609 *Molecular modeling and simulation of fusion-based amorphous drug dispersions*
610 *in polymer/plasticizer blends*, *European Journal of Pharmaceutical Sciences* 130
611 (2019) 260-268.
- 612 [8] B.D. Anderson, *Predicting solubility/miscibility in amorphous dispersions: It is*
613 *time to move beyond regular solution theories*, *Journal of pharmaceutical*
614 *sciences* 107(1) (2018) 24-33.
- 615 [9] I.M. de Arenaza, E. Meaurio, J.-R. Sarasua, *Analysis of polymer blends'*
616 *miscibility through molecular dynamics simulations*, *Polymerization* (2012) 29.

- 617 [10] S. Chang, X. Zhou, Z. Xing, Computing solubility parameters of phosphorus
618 flame retardants by molecular dynamics and correlating their interactions with
619 poly (ethylene terephthalate), *Textile Research Journal* 89(2) (2019) 195-203.
- 620 [11] M.B. Abderaman, E.-H.O. Gueye, A.N. Dione, A.A. Diouf, O. Faye, A.C. Beye,
621 A Molecular Dynamics Study on the Miscibility of Polyglycolide with Different
622 Polymers, *International Journal of Materials Science and Applications* 7(4)
623 (2018) 126.
- 624 [12] C. Wu, W. Xu, Atomistic molecular simulations of structure and dynamics of
625 crosslinked epoxy resin, *Polymer* 48(19) (2007) 5802-5812.
- 626 [13] M.S. Alam, J.H. Jeong, Thermodynamic properties and critical parameters of
627 HFO-1123 and its binary blends with HFC-32 and HFC-134a using molecular
628 simulations, *International Journal of Refrigeration* (2019).
- 629 [14] T.E. Gartner III, A. Jayaraman, Modeling and simulations of polymers: A
630 Roadmap, *Macromolecules* 52(3) (2019) 755-786.
- 631 [15] T. Spyriouni, C. Vergelati, A molecular modeling study of binary blend
632 compatibility of polyamide 6 and poly (vinyl acetate) with different degrees of
633 hydrolysis: an atomistic and mesoscopic approach, *Macromolecules* 34(15)
634 (2001) 5306-5316.
- 635 [16] C. Lavanya, K. Soontarapa, M. Jyothi, R.G. Balakrishna, Environmental friendly
636 and cost-effective caramel for congo red removal, high flux, and fouling
637 resistance of polysulfone membranes, *Separation and Purification Technology*
638 211 (2019) 348-358.
- 639 [17] W.E. Baker, C.E. Scott, G.-H. Hu, M. Akkapeddi, *Reactive polymer blending*,
640 Hanser Munich 2001.
- 641 [18] L.M. Robeson, *Polymer blends, A Comprehensive Review* (2007).
- 642 [19] M.T. DeMeuse, *High-temperature polymer blends*, Elsevier 2014.
- 643

- 644 [20] S. Shenvi, A. IPSMAil, A.M. Isloor, Enhanced permeation performance of
645 cellulose acetate ultrafiltration membranes by incorporation of sulfonated poly
646 (1, 4-phenylene ether sulfone) and poly (styrene-co-maleic anhydride), *Industrial*
647 *& Engineering Chemistry Research* 53(35) (2014) 13820-13827.
- 648 [21] P. Zhang, S. Xiang, H. Wang, Y. Wang, J. Zhang, Z. Cui, J. Li, B. He,
649 Understanding the multiple functions of styrene-co-maleic anhydride in
650 fabricating polyvinylidene fluoride hollow fiber membrane via coupled phase
651 inversion process and its effect on surface infiltration behavior and membrane
652 permeability, *Journal of Membrane Science* (2019) 117269.
- 653 [22] G.S. Ibrahim, A.M. Isloor, A.M. Asiri, A. IPSMAil, R. Kumar, M.I. Ahamed,
654 Performance intensification of the polysulfone ultrafiltration membrane by
655 blending with copolymer encompassing novel derivative of poly (styrene-co-
656 maleic anhydride) for heavy metal removal from wastewater, *Chemical*
657 *Engineering Journal* 353 (2018) 425-435.
- 658 [23] S.L. Mayo, B.D. Olafson, W.A. Goddard, DREIDING: a generic force field for
659 molecular simulations, *Journal of Physical chemistry* 94(26) (1990) 8897-8909.
- 660 [24] H. Meirovitch, Computer simulation of self-avoiding walks: Testing the
661 scanning method, *The Journal of chemical physics* 79(1) (1983) 502-508.
- 662 [25] D.N. Theodorou, U.W. Suter, Detailed molecular structure of a vinyl polymer
663 glass, *Macromolecules* 18(7) (1985) 1467-1478.
- 664 [26] D. Ongari, P.G. Boyd, O. Kadioglu, A.K. Mace, S. Keskin, B. Smit, Evaluating
665 charge equilibration methods to generate electrostatic fields in nanoporous
666 materials, *Journal of chemical theory and computation* 15(1) (2018) 382-401.
- 667 [27] X. Wu, B.R. Brooks, The homogeneity condition: A simple way to derive
668 isotropic periodic sum potentials for efficient calculation of long-range
669 interactions in molecular simulation, *The Journal of chemical physics* 150(21)
670 (2019) 214109.
- 671 [28] C.M. Hansen, *Hansen solubility parameters: a user's handbook*, CRC press2002.

- 672 [29] M. Zhang, P. Choi, U. Sundararaj, Molecular dynamics and thermal analysis
673 study of the anomalous thermodynamic behavior of poly (ether
674 imide)/polycarbonate blends, *Polymer* 44(6) (2003) 1979-1986.
- 675 [30] J.E. Mark, *Polymer data handbook*, (2009).
- 676 [31] C. Li, A. Strachan, Cohesive energy density and solubility parameter evolution
677 during thermoset curing, *Polymer* 135 (2018) 162-170.
- 678 [32] D. Paul, J. Barlow, H. Keskkula, Mark-Bikales-Overberger-Menges:
679 Encyclopedia of Polymer Science and Engineering, Vol. 12, John Wiley, New
680 York, 1988.
- 681 [33] S. Li, Z. Cui, L. Zhang, B. He, J. Li, The effect of sulfonated polysulfone on the
682 compatibility and structure of polyethersulfone-based blend membranes, *Journal*
683 *of membrane science* 513 (2016) 1-11.
- 684 [34] D.R. Paul, *Polymer blends*, Elsevier 2012.
- 685 [35] R. Fedors, D. Van Krevelen, P. Hoftyzer, C. In, *Handbook of solubility*
686 *parameters and other cohesion parameters*, Barton, AFM, CRC Press: Boca
687 Raton, FL, 1983.
- 688 [36] G. Brannock, J. Barlow, D.R. Paul, Blends of styrene/maleic anhydride
689 copolymers with polymethacrylates, *Journal of Polymer Science Part B: Polymer*
690 *Physics* 29(4) (1991) 413-429.
- 691 [37] A. Shulkin, H.D. Stöver, Microcapsules from styrene-maleic anhydride
692 copolymers: the study of morphology and release behavior, *Journal of membrane*
693 *science* 209(2) (2002) 433-444.
- 694 [38] A. Shulkin, Styrene-Maleic Anhydride, and Styrene-Maleimide Based
695 Copolymers as Building Blocks in Microencapsulation Procedures, 2002.
- 696 [39] Y. Aoki, Miscibility of poly (acrylonitrile-co-styrene) with poly [styrene-co-
697 (maleic anhydride)] and poly [styrene-co-(N-phenyl maleimide)],
698 *Macromolecules* 21(5) (1988) 1277-1282.

- 699 [40] K.S. Schweizer, J.G. Curro, Integral equation theory of the structure and
700 thermodynamics of polymer blends, *The Journal of Chemical Physics* 91(8)
701 (1989) 5059-5081.
- 702 [41] J.G. Curro, K.S. Schweizer, G.S. Grest, K. Kremer, A comparison between
703 integral equation theory and molecular dynamics simulations of dense, flexible
704 polymer liquids, *The Journal of Chemical Physics* 91(2) (1989) 1357-1364.
- 705 [42] K.F. Freed, New lattice model for interacting, avoiding polymers with controlled
706 length distribution, *Journal of Physics A: Mathematical and General* 18(5) (1985)
707 871.
- 708 [43] C.F. Fan, B.D. Olafson, M. Blanco, S.L. Hsu, Application of molecular
709 simulation to derive phase diagrams of binary mixtures, *Macromolecules* 25(14)
710 (1992) 3667-3676.
- 711 [44] F. Case, J. Honeycutt, Will my Polymers Mix?-Applications of Modelling to
712 Study Miscibility, Compatibility, and Formulation, *Trends in Polymer Science*
713 2(8) (1994) 259-266.
- 714 [45] M. Amini, M. Mobli, M. Khalili, H. Ebadi-Dehaghani, Assessment of
715 compatibility in Polypropylene/Poly (lactic acid)/Ethylene vinyl alcohol ternary
716 blends: relating experiments and molecular dynamics simulation results, *Journal*
717 *of Macromolecular Science, Part B* 57(4) (2018) 287-304.
- 718 [46] S.S. Jawalkar, S.G. Adoor, M. Sairam, M.N. Nadagouda, T.M. Aminabhavi,
719 Molecular modeling on the binary blend compatibility of poly (vinyl alcohol) and
720 poly (methyl methacrylate): an atomistic simulation and thermodynamic
721 approach, *The Journal of Physical Chemistry B* 109(32) (2005) 15611-15620.
- 722 [47] L. Feizhou, Z.-L. Lu, X.-s. Wang, Y.-t. Xi, A combined experimental and
723 molecular dynamics simulation study on *Eucommia ulmoides* gum's miscibility
724 with butadiene rubber, *Journal of Polymer Research* 24(7) (2017) 100.
- 725 [48] F.-Z. Li, Z.-L. Lu, D.-P. Tian, A Combined Experimental and Molecular
726 Dynamics Simulation Study on *Eucommia Ulmoides* Gum's Miscibility with
727 Several Rubbers, *Polymers and Polymer Composites* 25(1) (2017) 87-92.

- 728 [49] P.H. Brodsky, COMPATIBILITY IN POLYMER BLENDS, (1970).
- 729 [50] L.A. Utracki, B. Favis, Polymer alloys and blends, Handbook of polymer science
730 and technology 4 (1989) 121-185.
- 731 [51] J. Barlow, D.R. Paul, Polymer blends and alloys—a review of selected
732 considerations, Polymer Engineering & Science 21(15) (1981) 985-996.
- 733 [52] J.C. Mitchell, J.L. French, Analytical crucible, Google Patents, 2001.
- 734 [53] M. Padaki, A.M. Isloor, G. Belavadi, K.N. Prabhu, Preparation, characterization,
735 and performance study of poly (isobutylene-alt-maleic anhydride)[PIAM] and
736 polysulfone [PSf] composite membranes before and after alkali treatment,
737 Industrial & Engineering Chemistry Research 50(11) (2011) 6528-6534.
- 738 [54] J. Yoo, J. Kim, Y. Kim, C. Kim, Novel ultrafiltration membranes prepared from
739 the new miscible blends of polysulfone with poly (1-vinylpyrrolidone-co-styrene)
740 copolymers, Journal of membrane science 216(1-2) (2003) 95-106.
- 741 [55] Y. Wang, H. Song, H. Ge, J. Wang, Y. Wang, S. Jia, T. Deng, X. Hou,
742 Controllable degradation of polyurethane elastomer via selective cleavage of CO
743 and CN bonds, Journal of cleaner production 176 (2018) 873-879.
- 744 [56] T.R. Crompton, Thermal methods of polymer analysis, Smithers Rapra2013.
- 745 [57] J. Baker, An algorithm for the location of transition states, Journal of
746 Computational Chemistry 7(4) (1986) 385-395.
- 747 [58] K. Pajula, M. Taskinen, V.-P. Lehto, J. Ketolainen, O. Korhonen, Predicting the
748 formation and stability of amorphous PSMAI molecule binary mixtures from
749 computationally determined Flory– Huggins interaction parameter and phase
750 diagram, Molecular Pharmaceutics 7(3) (2010) 795-804.
- 751 [59] N. Wang, X. Huang, H. Gong, Y. Zhou, X. Li, F. Li, Y. Bao, C. Xie, Z. Wang,
752 Q. Yin, Thermodynamic mechanism of selective cocrystallization explored by
753 MD simulation and phase diagram analysis, AIChE Journal 65(5) (2019).
- 754 [60] B. Schneier, Polymer compatibility, Journal of Applied Polymer Science 17(10)
755 (1973) 3175-3185.

Supplementary Files

This is a list of supplementary files associated with this preprint. Click to download.

- [supplementaryfigures.docx](#)